STEEL GRIPS

JOURNAL OF STEEL AND RELATED MATERIALS

www.steel-grips.com

Products & Quality

GRIPS media GmbH
ISSN 1611-4442

2010

Mohammad R. Allazadeh:

Stresses introduced during cooling the as-cast steel slab

This paper discusses the major sources of residual stress generation in the steel microstructure during cooling process of as-cast steel (slabs, blooms, and billets). The stress configuration of the steel microstructure changes during quenching due to stresses introduced to the microstructure by these sources. The influence of each source in increasing the stress distribution within the microstructure during quenching is explained via corresponding formula and qualitative discussion in separate sections. The stresses accumulated during cooling may introduce the residual stress concentration zones in the microstructure of the steel. These stress concentration zones may result in flaws, microcracks or voids formation. Consequently, it may lower the soundness of the steel and cause deviation of the thermo-mechanical properties of the cast steel from the initially designed and customer desired specified properties.

Heat transfer in continuous casting steel, likewise other heat exchange processes, contains both heat transfers in the bulk as well as surfaces [1]. Fourier's law, Newton's law and Stefan-Boltzmann equation give the thermal energy transferred from the hot as-cast steel at secondary cooling zone by convection, conduction and radiation, respectively. The solidification of molten steel for each section of a slab ends in the secondary cooling zone at the so-called triple point in which the segregation from the side surfaces reaches the upper and lower surfaces' segregation. The extension of the triple point in the cooling symmetrical plane defines the centerline segregation in the slab. The temperature of the cast steel strand (T) at secondary cooling can be within the supercritical ($T > T$ [A_3] or T [A_{c3}]), intercritical (T [A_1] $< T <$ T [A_3] or T [A_{c3}]) or subcritical ($T > T$ [A_3] or T [A_{c3}]) temperature range. The temperature variation in the bulk of isotropic material undergoing cooling or heating process can be computed using overall balance of energy for a transient temperature gradient [2]:

$$k(T)\nabla T + \dot{q} = -\rho c\dot{T} \qquad (1)$$

Constants ρ and c are density and specific heat of material, respectively. The thermal conductivity of the body k depends only on temperature and, therefore, it can be moved out of the spatial derivative. The possible energy generated in the material is stored in $\dot{q}$. The negative sign is for reduction in the thermal energy.

The concepts in heat transfer have strong influences on the generation of stresses in the microstructure during cooling and limitations on optimum cooling rate for specific steel from a given temperature to ambient temperature. The efficient cooling rate for the slab is fundamentally controlled by the stresses generated in the microstructure during cooling. These stresses may develop to create voids or cause void growth. They may also form or propagate microcracks, flaws or cracks. Consequently, it is important to discuss in detail the stresses produced in the microstructure as a result of cooling the slab. The major stresses developed due to thermal, mechanical or phase transformation strains during the cooling stage of the as-cast steel are as follows:

a) thermal stresses,
b) volumetric stress,
c) internal stresses,
d) phase transformation stresses, and
e) post phase transformation stresses (interaction of phases).

In all cases, the stress level should reach the yield stress to develop inelastic strains on the slab surface or within its microstructure. The developed stresses due to cooling process should overcome the resistance of the material to plastic deformation, given by the Hall-Petch yield stress expression. This strength, in expanded form, is given as next [3]:

$$\sigma = \sigma_o + \Delta\sigma_S + \Delta\sigma_T + \Delta\sigma_P + \Delta\sigma_D + \kappa_y d_F^{-1/2} \qquad (2)$$

where σ is the Hall-Petch yield stress, σ_o is the lattice friction stress and $\Delta\sigma_S$ [4], $\Delta\sigma_T$ [5; 6], $\Delta\sigma_P$ [5], $\Delta\sigma_D$ [7] are the stresses corresponding to solid solution, texture, precipitation and dislocation effects, respectively. The last term in equation (2), $\kappa_y d_F^{-1/2}$ [6], is related to the ferrite grain size where, κ_y is the Hall-Petch constant and d_F is the ferrite grain diameter. However, the slabs have solidification (dendritic) structure, hence, the last term in the Hall-Petch expression does not apply to the as-cast slabs.

Any of these stresses, individually or in combination, beyond the inherent material strength can change the soundness of the final cast steel product during cooling process. These forces must overcome the adhesion forces between interfaces to separate the contact surfaces at the interface of two phases formed by austenite phase transformation within the microstructure or at interface of inclusions and steel matrix. The solid-solid phase transformation occurs within the microstructure during quenching the as-cast slab from the supercritical or the intercritical region. Therefore, phase transformation stress does not affect the stress distribution of the cast steel microstructure during quenching from subcritical temperature range. The following of this discussion elaborate to understand how each of these stresses is generated during quenching of as-cast steel.

Thermal stresses

Thermal stresses are generated from the poor thermal conductivity of the steel. This divides the slab into different temperature zones and, consequently, defines a thermal gradient through the thickness. Linear thermal strain for the thickness of each thermal zone is given by equation (3):

$$\delta_h = \alpha(\Delta T)L \qquad (3)$$

where α is the thermal linear expansion (contraction) and is different for each grade of steel. Onink et al. [8] measured the thermal expansion coefficient of ferrite β_α to be 1.75 · 10^{-5} K^{-1} for the temperature range 800 - 1200 K. However, the volumetric thermal expansion coefficient for each phase is not constant during cooling and it is temperature dependent. Metallurgists deployed the dilatometric method to calculate the thermal expansion coefficient for austenite [8] and martensite [9] as a function of temperature and atomic carbon fraction in % as follows:

$$\beta_\gamma = \left(24.9 - 0.5 \cdot C_\gamma\right) \cdot 10^{-6}, \tag{4}$$

$$\beta_{\mathrm{M}} = \left(14.9 - 1.9 \cdot C_{\mathrm{M}}\right) \cdot 10^{-6}, \tag{5}$$

where β_γ and β_{M} are the thermal expansion coefficients of austenite and martensite, respectively. The unit of both austenite and martensite thermal expansion coefficients is K^{-1}. C_γ and C_{M} are the atomic carbon fractions in % in austenite and martensite, respectively, and they can be calculated from the carbon mass contents in % in austenite and martensite which can be extracted from phase diagrams for each grade of steel. The conversion of mass contents to atomic fraction can be calculated using the next equation:

$$C_{\mathrm{A\%}} = \frac{\mathrm{C_{AW}} \cdot \mathrm{Fe_{W\%}}}{\mathrm{C_{AW}} \cdot \mathrm{Fe_{W\%}} + \mathrm{Fe_{AW}} \cdot \mathrm{C_{W\%}}} \cdot 100 . \tag{6}$$

Subscripts (W%), (A%) and (AW) stand for mass contents in %, atomic fraction in % and (AW) indicates the atomic mass of carbon and iron, respectively. In using equation (6), iron carbon microstructure has been considered because the summation of percentages should be 100 and other minor contamination can be neglected.

Therefore, a stress field is distributed at the interface of the thermal zone which, in turn, creates a region with compression stresses. These stresses increase the bending moment and, if it exceeds the yield strength of the steel slab, it may cause separation of the surfaces at the border of the thermal zone due to different thermal contraction in depth for each zone or microcrack or crack depending on the thermal gradient at the zone surfaces. Morris [10] explained how the changes in the steel temperature affects the Hall-Petch equation as well as ductile to brittle transition temperature. This alters the critical yield stress and the behavior of the transgranular crack. On the other hand, in the case of very high cooling rates, reheating of the middle section by the hot central section develops tensile stresses arising from the expansion of this section compared to a cooler layer above it which is in the stage of shrinking. If the level of tensile stresses developed in a region gets higher than the tensile properties of the slab steel, rupture in the texture may develop. As the temperature of the slab increases, the built-in thermal gradient in the microstructure gets bigger, so this type of stress distribution appears to be more effective in the supercritical region than in the subcritical region. Aketa and Ushijame [11] used the same logic for explaining crack formation due to thermal gradients during solidification process of the steel which has much higher temperature than just the torched off slab and, consequently, the thermal stresses are more pronounced in that temperature range.

Volumetric stress

The volumetric stresses are related to the heterogeneity of the microstructure due to presence of inclusions or other contaminant in the microstructure. Anomalies play a role in determining efficient cooling up to a certain level because of nucleation of stress concentration zones around the inclusions due to misfit contraction of two phases' material [12]. The influence of the presence of volumetric stresses in non-metallic inclusions on ductile fracture has been introduced by researchers via inclusion parameters. These parameters are total inclusion length per unit area or projected length P [13], inclusion mean free path Λ and nearest neighbour distance Δ [14], which are defined by equations (7), (8) and (9) respectively:

$$P = NA \cdot d , \tag{7}$$

$$\Lambda = \frac{2\sqrt{2}}{\pi} \left(1 - \frac{V_V}{P}\right), \tag{8}$$

$$\Delta = 0.349 \left(\Lambda S\right)^{1/3}, \tag{9}$$

where V_V is the inclusion volume fraction and $\overline{S}$ is the mean surface area of the particles.

Volumetric stress fields are generated during cooling since the material properties including volumetric thermal expansion (contraction) of the microstructure are different for different steels´ phase crystals as well as inclusions, voids and cracks. The relation between thermal stress and displacement between atoms due to changes in temperature is maintained by the thermal expansion coefficient in the stress-strain relationship. Equation (10) gives the coefficient of compressibility, β, in 1013.25 $mbar^{-1}$ whose value determines volumetric thermal expansion of the substance while the temperature is held constant [15]:

$$\beta = \frac{1}{V}\left(\frac{\partial V}{\partial P}\right)_T = \frac{\rho}{m}\left(\frac{\partial V}{\partial \rho}\right)_T \left(\frac{\partial \rho}{\partial P}\right)_T$$

$$= -\frac{\rho}{m}\frac{m}{\rho^2}\left(\frac{\partial \rho}{\partial T}\right)_T = -\frac{1}{\rho}\left(\frac{\partial \rho}{\partial P}\right)_T \tag{10}$$

where m is the atomic mass of the component. Equation (10) gives the relation between density, which is a material characteristic in a given boundary condition, and the rate of the temperature rise. Hence, different materials in a composite structure exposed to the same forces can be compressed at a different rate during cooling and this may cause separation between intermediate contact surfaces of two phases in contact or growing of the void or propagating the microcracks during the cooling process. Derivation with respect to temperature in equation (10) shows that volumetric stresses become less effective for quenching from the lower temperature range.

Internal stresses

Any arrangement of iron and carbon atoms other than perfect reference crystals may change certain steel properties, such as, thermodynamic, structural, scattering and chemical properties. It was reported that the density of cracks and distortion is higher as the carbon equivalent CE increases. The formula to calculate the value of CE is obtained from experimental results and it has been reported in the literature according to the alloying elements in the steel [1; 16]. The more common CE formula is as follows [17]:

$$C_{eq} = \%C + \left(\frac{\%Mn+\%Si}{6}\right) + \left(\frac{\%Cr+\%Mo+\%V}{5}\right) + \left(\frac{\%Cu+\%Ni}{15}\right). \quad (11)$$

The dislocations of the atoms form residual elastic stresses in the crystal. Therefore, dislocation density of the steel microstructure is a key point of the effect of existing internal stresses in selecting the proper cooling process. The disarrangement of atoms is studied in the course of the defects and is classified on the basis of the dimension of misalignment of atoms compared to their otherwise perfect position. The defects may fall in zero (point), one (line), two (area) or three (volume) dimension. As the dimension of the defect increases, its thermodynamic influence in the microstructure becomes more important. Generally, the defects by themselves are not very effective in the cooling process of the slab but the stress field around them can move by the dislocations and combine with other types of stresses embedded in the microstructure or generated during cooling. This may result in intensifying influences of the more effective stress fields in the cooling slab. In addition, the dislocation density is increasing as a function of stress field according to the following equation [10]:

$$n = \frac{q\ \pi\ L\ \tau_e}{G\ \boldsymbol{b}} \quad (12)$$

where G is the shear modulus, q is a geometric factor order unity and pile up length of the dislocation. The residual stresses are embedded in the effective shear stress τ_e and it increases as the number of dislocations increase. Then the dislocation density for mean grain size d can be calculated from a constant mean real boundary condition, cd^2, as shown next [10]:

$$\rho = \frac{N}{V} = \frac{cd^2}{d^3} = \frac{c}{d} \quad (13)$$

where N and V are the number of dislocations within the grain and the volume of the grain, respectively. c is a constant that depends on the shape of the grain. Consequently, the stored residual stress is related to the grain boundaries' density and properties. This fact can be deduced from the Hall-Petch equation as well and leads to one of the general errors in the numerical simulations of the localized behavior of the microstructure including crack behavior especially for irregular grain shapes like martensitic steels.

Phase transformation stresses

This is the most critical source of stresses generated during the cooling process. When the cooling curve passes the A_3 line in the Fe-FeC phase diagram, it experiences a solid-solid phase transformation which is completed with an isothermal process as the steel continues to cool below A_1. The start and end temperature of the transformation is determined using cooling curves such that the portion of curve where the transformation is occurring has a smaller slope and is characterized by an isothermal section in the curve, except for steel with eutectoid carbon content whose start and end transformation temperature is the same. During this transformation, the austenite phase with fcc structure transforms mainly to ferrite with the bcc unit cell structure in equilibrium cooling conditions, according to equation (14):

austenite [fcc] (0.8 % C) → ferrite [bcc] (0.02 % C) + Fe_3C [orthorhombic](6.67 % C). (14)

Fig. 1 shows the transformation of two unit cells of fcc to one unit cell of bcc. During this transformation, a homogeneous compression stress is applied in the direction of the arrows on the unit cells and an expansion stress is exerted in the plane normal to the compression stress. However, under non-equilibrium cooling conditions, austenite may transform to other phases such as martensite, acicular ferrite, bainite and other non-phase structures with special grain boundary structure. This transformation occurs with macroscopic distortion at invariant plane strain by a shear mechanism, which is called shape deformation or shape strain [18]. **Fig. 2** shows the transformation of the austenite unit cell with fcc structure to the bct martensite unit cell. This changes the lattice parameter and volume as well as the shape of the unit cell. The transformation is martensitic

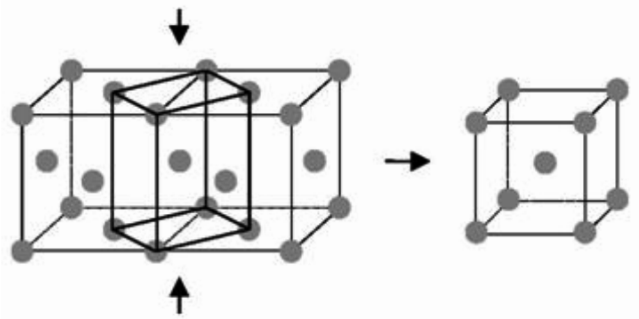

Fig. 1: Transformation of fcc unit cell to bcc unit cell

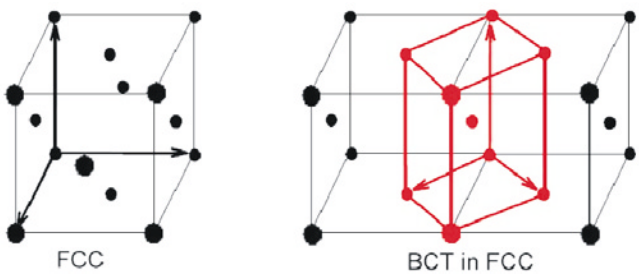

Fig. 2: Depiction of diffusionless transformation from fcc to bct during martensite formation

and the distortion is known as Bain distortion [18]. Application of small steps of Boger and Burgers types of homogeneous *shear* (B&B shear) shows that the Bain transformation is due to minimum energy path for homogeneous deformation [19]. The interested readers in martensitic transformation can find more information in [20]. The rate of phase transformation is given by well-known Avrami equation [21] as follows:

$$X_F = 1 - \exp\left(-ct^n\right) \tag{15}$$

where c and t are constants depending on temperature and are related to constant growth rate, nucleation frequency and shape factor. Rath [21] expanded the Avrami equation to a more general form of constant growth rate of the phase transformation as follows:

$$K_s G_o \left[t - t_o\right] = \alpha\left[\left(X_V\right)^{1-n} \left\{\frac{1}{1-n} + \sum_{K=1}^{\infty} \frac{B}{1+K-n}\left(X_V\right)^K\right\}\right] + \beta\left[-\left(1-X_V\right)^{1-m}\left\{\frac{1}{1-m} + \sum_{K=1}^{\infty}\frac{B'}{1+K-m}\left(X_V\right)^K\right\} + \gamma\right] \tag{16}$$

where $a = 1$ and $b = 0$ for $0 \le X_V \le 0.5$ and $a = 0$ and $b = 1$ for $0.5 \le X_V \le 1.0$. K is an index integer and m and n do not have simple shape and their values are presented in several papers.

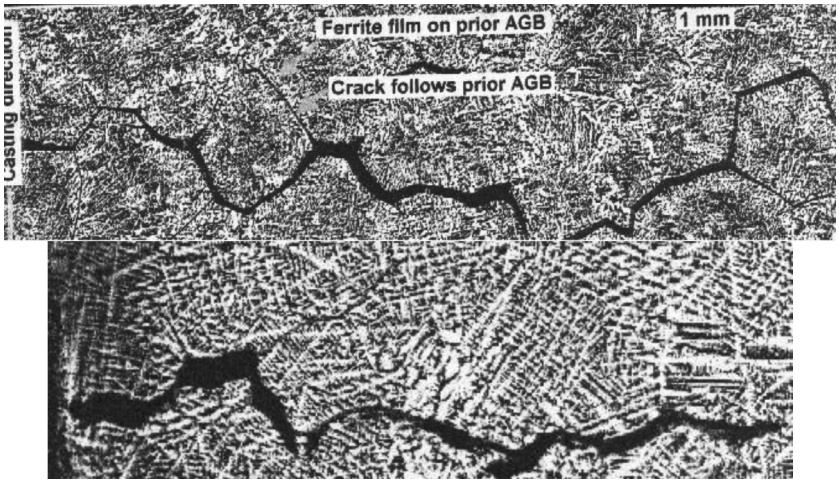

Fig. 3: Crack propagation along a ferrite film on prior austenite grain boundaries [23]

Recently, some of the researchers [9] suggested a conversional model based on the relative atomic volume change occurring during the phase transformations and change in solute atoms in the matrix to predict the volume fraction in low-alloy steels. They claimed that this method could be used for estimating the volume fraction of ferrite, pearlite, bainite and martensite at room temperature using the lattice parameter of each phase as a function of temperature and solute content. The geometry of a unit cell and, consequently, the crystal built by these unit cells change during the cooling process either under equilibrium or non-equilibrium conditions indicated on the iron-carbon phase diagram. Therefore, this type of stress can be called geometrical stress, which is the consequence of a dilatational strain introduced to the matrix by the transformation process. Some inequalities [9] suggested dilatometric tests for determining the start and end temperature of phase transformation by constant monitoring of dimensional change during a heat treatment process. However, since the lattice parameter and, as a result the volume of the unit cell, changes during the transformation, phase transformation also produces the volumetric stresses in the microstructure. This combination of geometrical stresses and volumetric stresses creates a strong stress distribution at the grain boundaries, which may result in the cracks along the grain boundaries at the softer phase region.

Researchers have also reported the segregation of ferrite network at weak prior austenite grain boundaries (AGB) [23] and at oscillation marks on the continuously cast steel strand [24; 25] as a source of crack formation during eutectoid transformation. Tsai and his coworkers [23] were able to take photos of the cracks due to the eutectoid transformation. **Fig. 3** shows these photos indicating the cracks along the prior austenite grain boundaries in a ferrite film.

Phases interaction induces stresses

Each phase has its own material properties including thermal properties. It can be observed in the phase diagram that the supercritical region has only austenite phase microstructure whereas the microstructure of the intercritical region consists of two phases of ferrite and austenite. However, the subcritical region can have a steel structure with more than two phases depending on the cooling rate and cooling process. The type and fraction of the phases at each temperature within the subcritical temperature region can be deduced from TTT and CCT diagrams. These phases create an inhomogeneity in the microstructure from the material property point of view. The lattice parameter of each phase changes differently with temperature drop during cooling. Researchers have implemented the dilatometric method. They calculated the changes in the lattice parameter as a function of temperature and thermal expansion. Next equation calculates the lattice parameter during cooling or heating ferrite as following [8]:

$$\alpha_\alpha = 0.28863\left\{1 + \beta_\alpha\left(T - 800\right)\right\}, \tag{17}$$

and for austenite is [8]:

$$a_\gamma = \left(0.36306 + 7.83\cdot 10^{-4}\cdot C_\gamma\right)\left\{1 + \beta_\gamma\left(T - 100\right)\right\}, \tag{18}$$

and for martensite is [9]:

$$a_M = (0.28610 - 0.0002898 \cdot C_M)\{1 + \beta_M (T - 273)\} \quad (19)$$

$$c_M = (0.28610 - 0.00028558 \cdot C_M)\{1 + \beta_M (T - 273)\} \quad (20)$$

β_α is $1.75 \cdot 10^{-5}$ K^{-1} and β_γ and β_M are defined by equations (4) and (5), respectively. Constants C_γ and C_M are given by equation (6). C_γ varies with temperature and C_M depends on the quenching process. The lattice parameter of cementite is only temperature dependent and is given by the next formulae [26]:

$$a_{Fe_3C} = 0.45234\left\{1 + \left(5.311 \cdot 10^{-6} - 1.942 \cdot 10^{-6} T + 9.655 \cdot 10^{-12} T^2\right)(T - 293)\right\}, \quad (21)$$

$$b_{Fe_3C} = 0.50883\left\{1 + \left(5.311 \cdot 10^{-6} - 1.942 \cdot 10^{-6} T\right) + 9.655 \cdot 10^{-12} T^2\right)(T - 293)\right\}, \quad (22)$$

$$c_{Fe_3C} = 0.67426\left\{1 + \left(5.311 \cdot 10^{-6} - 1.942 \cdot 10^{-6} T\right) + 9.655 \cdot 10^{-12} T^2\right)(T - 293)\right\}. \quad (23)$$

The units of all lattice parameters in the above equation, are in nanometers and the equations were verified by researchers' results. This produces a volumetric stress field during cooling of the slab and, consequently, can introduce new microcracks in the microstructure or propagate existing cracks.

Conclusion

Quenching of cast steel strands (slabs, blooms, and billets) changes the stress configuration of the microstructure. Five major sources of stresses were discussed in this paper and their roles in altering stress distribution in the microstructure were explained. Although all five sources of the stress generations listed in this paper increase the residual stress of the microstructure, in comparison to solid-solid phase transformation, other sources of stress generation influence the stress configuration on a smaller scale. It is important to study the sources which induce residual stresses during cooling process since the formation of the stress concentration zones in the microstructure of the steel may result in flaws, microcracks and voids formation. This lowers the soundness of the steel which may cause diverting the thermomechanical properties of the steel from the initially designed properties. Therefore, it is important to take into the consideration the stress sources during quenching in designing cooling process, numerical calculation of cooling rate and computer simulation of cooling cast steel.

References

[1] Pehlke R. D.: Heat Transfer I; Short course on Continuous Casting, 33rd Electric furnace conf., Houston, Texas, Dec, 1975.
[2] F. P. Incropera, D. P. DeWitt: Fundamentals of Heat and Mass Transfer, 6th edn., Willey and Sons, 2006.
[3] J. D.; Preston R. R.: Processing and Properties of Low Carbon Steels, J. Gray, [ed.:], American Institute of Mining, Metallurgical, and Petroleum Engineers, 1973, p. 1.
[4] Pickering F. B.: Physical Metallurgy and the Design of the Steels, Applied Science, London, 1978, p. 140.
[5] Gladman T., Dullieu D., Mclvor I. D.: Microalloying 75, M. Korchynsly et al., [eds.:], Union Carbide Corporation, 1977, p. 32.
[6] Backofen W. A.: Deformation Processing, Addison Wesley, 1972, p. 57.
[7] Dieter G. E.: Mechanical Metallurgy, 3rd edn.,. McGraw-Hill, 1986, p. 471.
[8] Onink M., Brakman S. M., Tichelaar F. D., Mittemeijer E. J., Van der Zwag S.: Scripta Mater. 29 (1993), p. 1011.
[9] Lee S. J., Lusk M. T., Lee K. Y.: Acta Mater. 55 (2007), p. 875/82.
[10] Morris Jr., J. W.: The Influence of Grain Size on the Mechanical Properties of Steel, Proc. Intern. Symp. Ultrafine Grained Steels, S. Takaki and T. Maki, [eds.:] Iron and Steel Inst. Japan, Tokyo, 2001, p. 34/41.
[11] Aketa Y., Ushinjama K.: Tetsu-To-Hagané 46 (1960), p. 1733.
[12] Allazadeh M. R., Garcia C. I., DeArdo A.J. and Lovell M. R.: Journ. ASTM Intern. 6 (2009) No. 5, Paper ID: JAI102041, DOI: 10.1520/JAI102041.
[13] Tossoll A., Berdin C., Prioul C.: Int. J. Fract. 15 (2002), p. 205.
[14] Spitzig W. A.: Metall. Trans. 14A (1983), p. 271.
[15] DeHoff R. T.: Thermodynamics in materials science, McGraw Hill, 1993, p. 43.
[16] MacKenzie D. S.: Advances in Quenching- A Discussion of Present and Future Technoligies, Heat Treating and Surface Engineering, Indiana, USA, Sep. 2003, p. 184/91.
[17] Gomez M., Garcia C. I., Haezebrouck D. M., DeArdo A. J.: Compositional Design Concepts Using Al and Si as Alloying Elements in TRIP Steels, Intern. Conf. Microalloyed Steels: Processing, Microstructure, Properties and Performance, Iron & Steel Technology, July, 2007, p. 267/76, Pittsburgh, Pennsylvania, USA.
[18] Wayman C.M.: Martenistic transformations: an overview, Pittsburgh, USA, ASM Phase Transform. Commit., 1981, p. 1119/44.
[19] Beachamp P., William J.P.: Computer determination of minimum energy path in the bcc-fcc transformation by homogeneous deformations, Pittsburgh, USA, ASM Phase Transform. Commit., 1981, p. 1221/25.
[20] Material Science Forum, Vol. 3, 1985.
[21] Askeland D. R., Phule P. P.: Essentials Of Materials For Science And Engineering, Thomson Learning, Andover, UK, 2004 edn.
[22] Rath B. B.: The overall kinetics of isothermal transformations, Pittsburgh, USA, ASM Phase Transform. Commit., 1981, p. 1097/103.
[23] Tsai H. T., Yin H., Lowry M., Morales W.: Iron & steel Technol. (2006) July, p. 23/31.
[24] McPherson N. A., Mercer R. E.: Ironmak. Steelmak. (1980) No. 4, p. 167/79.
[25] Harada S. et al.: ISIJ Intern. 30 (1990) No. 4, p. 310/16.
[26] Stuart H., Ridley M.: J. Iron & Steel Inst. (1970) May, p. 469.

Mohammad R. Allazadeh
Ph.D.
Institute of Mechanical Engineering
University of Pannonia
Veszprem, Hungary